JOURNAL OF SPACECRAFT AND ROCKETS
Vol. 29, No. 5, September-October 1992

Rapid Method of Calculating the Orbital Radiation Environment

Michele M. Gates* and Mark J. Lewis†
University of Maryland, College Park, Maryland 20742
and
William Atwell‡
Rockwell International, Houston, Texas 77058

This paper describes the process of integrating available environment models into a single package to calculate the radiation environment for any Earth orbit quickly and accurately with the only input being initial orbit parameters, launch date and length of mission, and units of output. The radiation dose is calculated for particles penetrating varying aluminum shielding thicknesses and incident upon several materials inside. Included also are modifications that have been made to the codes that account for the decrease of the magnetic field with time, which allows the use of data taken in the past to accurately predict a future environment. The complete package has relatively short run times, on the order of a few minutes on either a PC or MicroVAX II, allowing multiple iterations for application to mission design and planning.

Introduction

PLANNING for the radiation environment of a spacecraft is essential for the mission's success. This is especially true in planning manned missions, both orbiting and interplanetary. Charged particles can penetrate electronic parts, depositing their energy, sometimes up to several hundred mega electron volts, causing them to fail, both temporarily and permanently. In addition to concern about part failures, manned mission analysts must anticipate human exposure. Radiation exposure to astronauts and aircraft passengers can cause temporary and permanent injury to the skin, lungs, pancreas, intestines, liver, heart, and other vital organs. The radiation dose for tissue can be modeled as dose in very thin water layers, which is incorporated into this work, or it can be measured in the units of blood-forming organ (BFO) dose, which is not currently incorporated.

All of these concerns make defining the radiation environment for each specific orbit an extremely important aspect of each of the mission planning processes. For example, for electronic parts analysis, information is desired on the radiation dose in rads-silicon; life support is concerned with the dose in water; other equipment and structures designers may be interested in the dose in aluminum; and ideally this information should be available in the initial planning stages of a mission. Unfortunately, radiation modeling in the past has proven to be a costly and lengthy process, not amenable to premission planning and design analysis. It would be most desirable to have depth-dose curves (dose vs shielding thickness) for many orbits of choice—of several varying altitudes, inclinations, and mission lengths—so that both cost and safety analyses could be made early in the planning process.

Presented as Paper 91-0098 at the AIAA 29th Aerospace Sciences Meeting, Reno, NV, Jan. 7-10, 1991; received May 8, 1991; revision received Feb. 19, 1992; accepted for publication Feb. 19, 1992.

*Research Assistant, Department of Aerospace Engineering. Student Member AIAA.

†Assistant Professor, Department of Aerospace Engineering. Member AIAA.

‡Senior Staff, Space Systems Division—Houston Operations. Member AIAA.

The trapped radiation environment consists of protons, electrons, helium, carbon, oxygen, and other ions trapped in the Earth's magnetic field. It is important to remember that the models used in this study are proton and electron models, though the proton model represents contributions from many ion species that have not been individually identified. These particles originate from the sun, cosmic rays, and the Earth's plasma sheet and ionosphere. The particles enter the trapping region of the magnetosphere and are continually deflected by the magnetic field lines and reflected near the poles, forming the trapped radiation belts.[1]

The three-dimensional shapes that the dipole field lines construct approximate the L-shells (McIlwain drift shell parameter), which are defined by the equations of motion of particles in the field, which run tangent to the field lines. The L value is defined to be the distance, in Earth radii, of a particular L shell from the center of the Earth in the equatorial plane. The L value and the local magnetic field intensity, B, construct the McIlwain geomagnetic coordinate system.[1,2]

The magnetic field is modeled statically but is in reality a highly dynamic system. The field strength is decreasing with time, about 16 nt per year on average, and drifting westward at a rate of about 0.27 deg per year. Since the field strength is decreasing with time, the particles trapped in the field lines move with the field (closer to the Earth). The field also changes with the solar cycle, expanding during periods of low solar activity (solar minimum) and contracting during active times (solar maximum). In addition, a solar flare event will cause the field to contract further, pushing the field to lower latitudes, altering the shape of the system and exposing more of the polar latitudes to the free-space environment. Many more variations exist, but a complete discussion is beyond the scope of this work.

The radiation belts are contained by the magnetic field; consequently, as the magnetic field changes, the belts vary in response. Magnetic storms also change the particles' direction and energy. These conditions must be kept in mind when using the models, and room for variance should be allowed. The trapped particle environment was mapped out on several spacecraft flights, including several Explorer, Injun, and Gemini missions. These measurements were taken in the 1960s, at a time when the trapped environment was different than it is now. The treatment of these variations with time will be explained in the subsequent section.

Solar protons travel from the sun in the solar wind at velocities that vary from 275 km/s to over 1000 km/s after an extremely severe solar flare. During and directly after the occurrence of a flare, the protons arrive at the Earth in large quantities, sometimes greater than 1.0×10^{10} particle/cm^2 and at energies sometimes above the giga electron volt level. The free-space integral fluence for a 5-yr mission during a solar maximum is typically predicted to be on the order of 1.5×10^{11} particle/cm^2 (Refs. 3, 4). On the average, the solar cycle is an 11-yr cycle, with 5½ yr in solar minimum and 5½ yr in solar maximum, with the midyears of each being either the most quiet or most active periods. Unfortunately, there is currently no method of predicting the occurrence of a flare or its composition. This problem can only be treated with a probabilistic approach, two of which are outlined later. There is much concern about solar flare protons, especially given the recent high solar flare activity and several resulting satellite anomalies.

The magnetic field provides an impedance against charged particles originating in free space. This impedance increases toward the Earth, distorting the paths of the protons and preventing their penetration of the field. Each L shell has a characteristic cutoff energy at which protons at and below the energy level cannot penetrate. The cutoff energy increases toward the Earth, allowing only higher energy protons to penetrate deep into the field. This phenomenon is called geomagnetic attenuation.

Integrated Dose Package

Available Fortran programs were used in the modeling, which currently runs on a MicroVAX II in about 20 min. Existing codes have been modified to include the changes in the environment with time, allowing a more accurate prediction of the environment for future missions.

To model the complex orbital environment for a given space mission, the orbit is calculated first. The position in space must be known in small enough intervals to calculate the particle fluxes/fluences and integrate them over the orbit. Since the orbit will usually change with time, passing over many places on the Earth as it rotates beneath the orbiter, an orbit-averaged flux/fluence over a large number of orbits will give a good overall total sampling with which to calculate the total dose. Typically, the position of the orbiter is calculated every minute for 40 orbits in the mission. Note that if precession over a long period of time is to be taken into account, the sampling is chosen over appropriate precessing conditions.

The trapped particle environment data consist of extensive files with measured particle energies and fluxes stored in arrays already incorporated into the model used in this work, which will be explained in the following section. For each of the orbit points, the particle energy spectrum is scanned, with the flux at each of the energy levels being returned. The particle code incorporated performs the orbit-averaging calculations.

The free-space solar proton fluence is calculated for the entire mission time. The magnetic field provides an impedance to these particles, eventually stopping them. The geomagnetic cutoff can be calculated around the orbit at each of the points previously calculated in geocentric coordinates. Knowing the magnetic cutoff at each point in the orbit, a percentage of total fluence of each energy that reaches the spacecraft is calculated and applied as an addition to the radiation environment.

At this point, the environment outside of the spacecraft is known. Some of the particles will penetrate the aluminum and irradiate the materials inside. The package incorporates a shielding code, which calculates the radiation dose on materials in varying thicknesses of aluminum. The dose is determined in the units of the material in the shielding: rads-water, -silicon, -aluminum, and -silicon dioxide.

Integrating these codes together consists of writing a driver program and short subroutines to link the codes together. They can be run continuously with a Digitial Equipment Company Command Language (DCL) command file, or some equivalent. Figure 1 describes the individual program in the Integrated Dose Package with a flow chart. Note that the only input parameters needed for the completed model are initial orbit parameters, launch date, time of mission, solar conditions, and the dose units of output and that all of the calculations are done internally, with the output being the total dose data. The output of any of the programs included is available, such as the doses, orbit calculations, solar proton fluences, and trapped particle fluxes.

Method of Calculation—Orbit Calculations

The orbit integration code that is incorporated in this work is the ORBIT package.[5] The initial orbit parameters are input, such as the altitude of apogee and perigee, inclination, perigee displacement to initial position, argument of perigee, right ascension of ascending node, and precession values, if desired. The ORBIT code calculates points along the trajectory in geocentric coordinates (altitude, latitude, and longitude) in 1-min intervals for 40 orbits. A large number of orbits usually give sufficient sampling of the environment with which to perform a good average.

As previously mentioned, the field itself is decreasing with time and drifting westward. To calculate the trapped particle fluxes, the models of the magnetic field used correspond to the same years that the trapped particle data were measured. The magnetic field models IGRF1965, for solar minimum conditions, and Hurwitz 1970, for solar maximum conditions, find the geomagnetic coordinates in B and L values corresponding to each of the geocentric data points. These models are used in this work because they have been deemed to be the most accurate approach and have been verified with Shuttle dosimetry measurements.[6,7] The models are run for input years at which the solar maximum and minimum occurred in this time period—1964 for solar minimum conditions and 1970 for solar maximum conditions. This procedure allows a calculation of the environment as it was at the time that the data were taken.

To account for the decrease in the field strength with time, the dipole moment is modified. The dipole moment is recalculated for the solar minimum and solar maximum conditions for the time of the mission to project the field into the future. This is done with the use of the following equation:

$$M = \sqrt{G_{12} + G_{22} + G_{21}} \times 10^{-5} \quad (1)$$

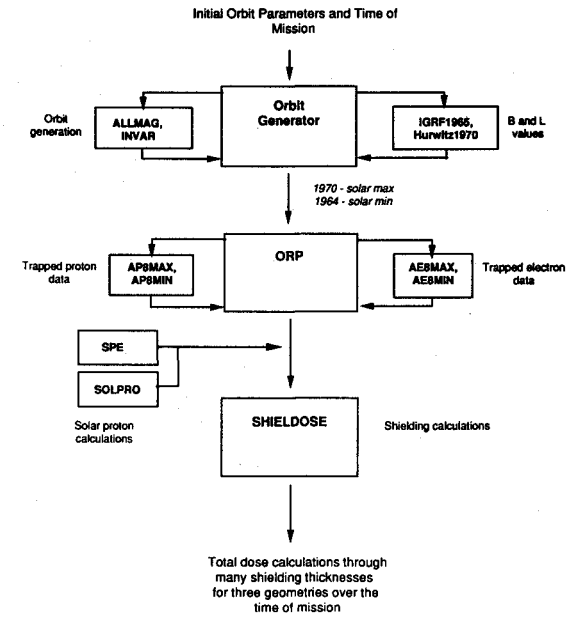

Fig. 1 Structure of the Integrated Dose Package, showing the interaction of the assembled individual software components.

where M is the dipole moment, in Gauss, and G_{nm} are the field expansion coefficients from the IGRF1985 data set.[8]

This method does not account for the westward drift of the magnetic field, which most dramatically manifests itself in the South Atlantic anomaly. The drift is about 0.27 deg/yr westward, so an orbit averaging is done or the data from a given analysis can be corrected by shifting the field accordingly from the date of the model used.

Since the solar proton models represent current data, the magnetic field model corresponding to the current time, currently IGRF1985, is used for the geomagnetic attenuation.

In times of increased solar flare activity, the field is compressed downward in latitude, which can leave more of the polar region exposed. This effect has not been taken into account in the models, since they are strictly static models.

Trapped Radiation Data

Trapped radiation data for this work were obtained from the AP8 and AE8 models, which represent the most current data readily available, including separate models for both solar maxima and minima.[9,10] The proton and electron energies and fluxes are stored in arrays indexed by geomagnetic coordinates, i.e., B and L values. To access the data, the points in the orbit previously calculated as altitude, latitude, and longitude are now converted to B and L . For the energy spectrums, the ORP code accesses the data sets for each of the geomagnetic coordinate points and the dipole moment previously calculated. Because the data for these models were taken at specific points in space, exponential interpolation is performed between the points to find the flux at the exact coordinates specified. An orbit-averaged flux is then determined after the fluxes corresponding to all of the orbit points have been calculated.

Because the magnetic field models for the correct time period were used, the trapped environment has been accurately calculated for the years that the AP8 and AE8 data were taken. Since the field is drifting westward, an orbit-averaged flux should be used to project the flux to future mission times.

Solar Proton Models

Both the solar proton events (SPE) model and the SOLPRO model were used in this work.[3,4,11] The SPE model contains data from three solar cycles, which is three times longer than the data sets used in previous models. The model is time dependent, taking as input the date and length of a mission and the confidence level, and predicts the fluence based on which years are spent in the active periods. No distinction is required between "ordinary" and "anomalously large" events and the calculation is done for any specified energy above 10 MeV. In addition, the period considered hazardous for enhanced proton fluences was found to be 7 yr. During the September and October 1989 solar flares, energies of several hundred mega electron volts were recorded, making this type of capability particularly useful. A modified SPE model contains the data from these 1989 flares.

The SOLPRO model depends on the length of time spent in solar max, up to 6 yr, and the confidence level to be considered and calculates fluences for energies up to 100 MeV, which could be extrapolated to larger energy levels. The model calculates fluences corresponding to the predicted number of anomalously large and ordinary flares separately. Extremely large events, such as the August 1972 flare, are considered to be anomalously large, and more typical events are considered to be ordinary.The SOLPRO model has been used extensively in this type of calculation in the past.

Having both solar proton models integrated has an important advantage. First, the outputs of each solar proton model are compared for the same energies and mission specifications. Then a more complete analysis can be done using the SPE model for a larger range of energies. In general, the two models compare favorably in particle spectra, although the SPE model predicts a higher fluence in the more active years.

Both of these models calculate the integral free-space fluence for the solar proton energy specified. For the shielding program and attenuation process described later, the integral fluences (particle/cm^2) are converted into differential fluences (particle/cm^2-MeV).

Geomagnetic Attenuation

The geomagnetic cutoff for solar protons is treated by using the B and L coordinate system. In this process, the most recent magnetic field model, IGRF1985, has been used to compute the B and L values for each point previously calculated in geocentric coordinates. This is not to be confused with the magnetic field models used for the trapped particle environment. Since the solar models predict present conditions, current magnetic field models are used. The objective is to find the daily percent of time spent near specific L shells. This is done by calculating the amount of time spent in small L bins, such as $L = 1.2$–1.4 and $L = 5.4$–5.7. The mean L value of each small L bin is then found, and the cutoff energy for the small L bin estimates the cutoff energy of the mean L value. The percent of time spent in the accessibility range of a proton is approximated by the percent of time spent in L bins with a cutoff energy at or below the energy of the particle.

The total attenuated fluence for each energy is the product of the free-space differential fluence times the percent of the time spent in the accessible range for that energy.

Shielding Codes

The shielding code SHIELDOSE is one that is readily available, is relatively easy to operate, and has been used extensively in the field.[12] The electron calculations make use of a modified Monte Carlo code and are accurate to within 10–20% of experimental dosimetry testing, although boundary effects, such as those at a corner or on the edge of a slab, can drop that accuracy to 30%. The proton calculations were performed using the straight-ahead, continuous-slowing-down approximation that includes coulomb interactions but neglects nuclear interactions. The code described uses transport coefficients for an aluminum material but allows a choice of the material that the radiation will be incident upon after penetration of the aluminum. The deposited energy (dose) is calculated for three geometries—finite slab, semi-infinite medium, and solid sphere—through specified aluminum shielding thicknesses. The units of choice are rads-aluminum, -silicon, -water, or -silicon dioxide, which specify the material behind the shielding. A rad is a unit specifying the amount of energy deposited in a material and is equal to 100 erg/g = 1.602×108 MeV/g = 10^{-2} Gy (Gray). The dose in rads-water is the calculated dose in very thin water layers (tissue equivalent).

It should be noted that these geometries are idealized and may not be present in the actual design configuration. The real case would most likely lie somewhere between the semi-infinite slab and solid sphere geometries, depending on the location of the point of interest in the complete real geometry. If the area in question is located directly behind a long slab of aluminum and far from the edge with radiation incident from a direction opposite the slab, the point would lie close to the slab curve. However, if the point in question were near the edge of the slab or at the center of a spherical surface, the solid sphere geometry would be more appropriate.

When penetrating the aluminum shielding, the electrons interact with the aluminum atoms, producing secondaries such as bremsstrahlung photons and secondary electrons that continue to penetrate and can also have an effect on the material inside. The effects of electron interaction with the aluminum nuclei, including bremsstrahlung photons, multidirectional deflecting, and backscattering, are calculated by the SHIELDOSE code, but the effects of secondary neutrons produced in proton reactions with the aluminum nuclei are not included. Because SHIELDOSE does not include proton secondary ef-

fects, the PDOSE code from Johnson Space Center was used to compare solar proton doses.

The contributing radiation sources, including trapped protons, solar protons, trapped electrons, and bremsstrahlung, are calculated, and then integrated for the total dose of the mission. The output is in tabular form that can be integrated with a graphics package to give instant dose-depth curves for each component and the total radiation dose.

Results

The total dose output for a polar orbit (98.2 deg) at 700 km is shown graphically in Fig. 2. The curve shows the contributions to the total dose and the integrated (total) dose. Note that the electron component drops off rapidly at about 1 gm/cm^2 and that the protons, both trapped and solar, are almost the sole contributors beyond this point. Also, though the bremsstrahlung radiation is a secondary effect of the electrons, the bremsstrahlung component of the dose does not disappear with the electron component; instead, it continues to propagate far beyond the electrons, surpassing it around 2.5 gm/cm^2. This phenomenon can be particularly important for those orbits containing little or no trapped or solar protons, where the bremsstrahlung will be the only component of the dose at high shielding thicknesses.

Figure 3 presents another part of the direct output from the package. The three geometries are plotted together for comparison. The solid sphere clearly has the highest radiation dose behind its shielding, although the shape of all three curves is the same. The semi-infinite medium and finite slab are very close to each other, except at lower shielding thicknesses, where they can differ considerably. It is important to note that the geometries given are ideal for calculation and are usually not present in the actual design configuration. For this reason, the solid sphere geometry curve is usually chosen for design considerations, since it represents a worst-case scenario. None of these calculations have a safety factor included. This must be determined separately.

To compare the output of this package with other analyses of the same type, the code was run for a 700-km (98.2-deg) orbit for 5 yr during solar maximum. Calculations done by the Jet Propulsion Laboratory (JPL) and General Electric (GE) were provided for comparison. The highest differences occurred at very low shielding thicknesses, around 0.01 gm/cm^2/Al, where both GE and the Integrated Dose Package calculated $\simeq 3.3 \times 10^8$/rads-Si and JPL's results showed $\simeq 2.2 \times 10^8$/rads-Si. The three curves were within 10% elsewhere. One possible reason for the slight differences present is the difference in launch dates used for each analysis. JPL considered a launch date in March 1997, GE used 1995, and this work used June 1998.

With this package, calculations can be done for different orbits to both qualitatively and quantitatively analyze the

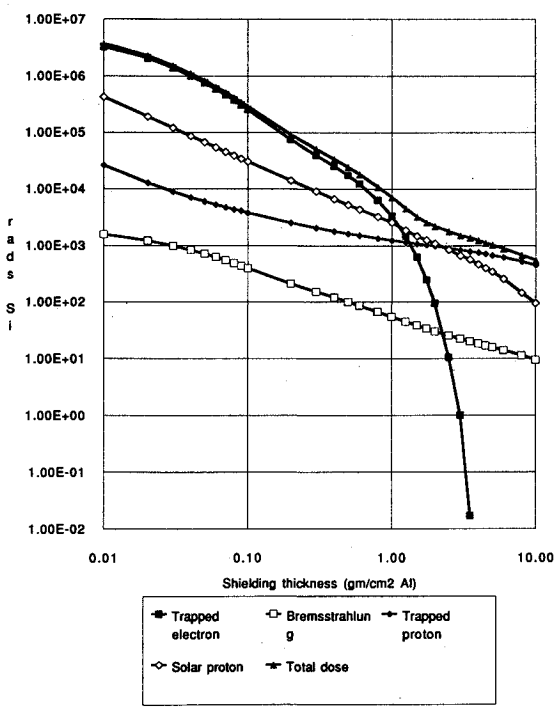

Fig. 2 Total dose results in a silicon target inside a solid aluminum sphere for a 5-yr polar orbit (98.2 deg) at 700 km in solar maximum.

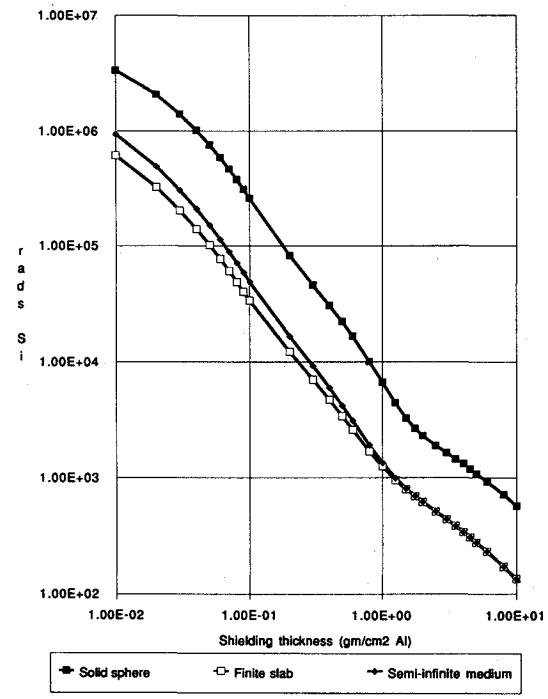

Fig. 3 Total dose calculated in silicon target for finite slab, semi-infinite medium, and solid sphere aluminum geometries in a 5-yr polar orbit (98.2 deg) at 700 km in solar maximum.

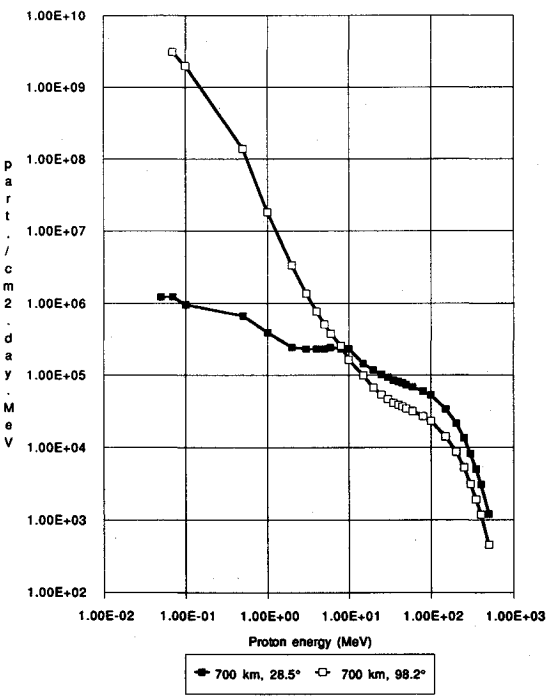

Fig. 4 Trapped proton orbit-averaged differential flux for a 700-km orbit at two different inclinations, 28.5 and 98.2 deg at solar maximum.

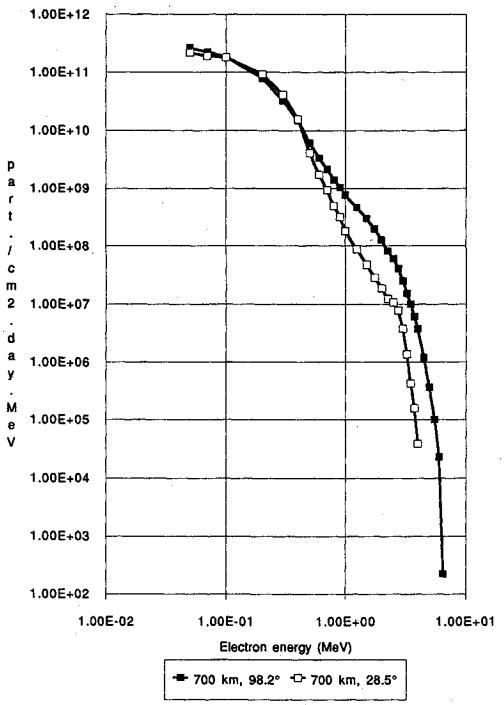

Fig. 5 Trapped electron orbit-averaged differential flux for a 700-km orbit at two different inclinations, 28.5 and 98.2 deg at solar maximum.

radiation environment as a whole. Figure 4 presents the trapped proton differential flux for a 700-km orbit at two different inclinations: 28.5 and 98.2 deg. The curves show that the flux of 10 MeV particles is very close at these inclinations, up to four orders of magnitude different at lower energies, such as 0.1 MeV, and significantly different at the higher energy levels, such as 100 MeV. Figure 5 shows the trapped electron differential flux for the same scenario. There is not much difference at the low electron energies, such as 0.1 MeV, but at the higher energies, the differences begin to grow; at 1 MeV the difference is a factor of 4. The difference in the solar proton dose for the two conditions is shown in Fig. 6. Here, the shape of the curves is identical, but the magnitude of the dose in polar orbit is three orders of magnitude higher than the dose in the 28.5-deg orbit.

The total dose for the two scenarios is compared in Fig. 7. The dose at low shielding thicknesses is almost unaffected by the change in inclination, which is due to the relatively consistent electron flux distribution, since the electron contribution affects the lower shielding end of the dose curve. At the middle shielding thicknesses, the dose is significantly different for the two inclinations. This aspect is due to the difference in the solar proton dose, shown in Fig. 6, which is most prevalent in the shielding thicknesses above which the electron contribution drops off, as is shown in Fig. 2. It should be noted that the geomagnetic cutoff has been calculated, but the Earth's shadow and geomagnetic conditions are not included. The results shown in this graph indicate the utility of the Integrated Dose Package in combining information already available to achieve both qualitative and quantitative radiation dose estimates as a prelude to mission planning.

The solar proton doses calculated by the SHIELDOSE and PDOSE codes are compared in Fig. 8. The two codes exhibit excellent agreement for shielding thicknesses greater than 0.2 gm/cm^2, although for thinner shielding, the SHIELDOSE results are significantly below those of PDOSE. This is primarily due to the lower energy limit in the solar proton spectra, 10 MeV, which has a range of approximately 0.2 gm/cm^2 in aluminum. The PDOSE code does a semilog interpolation back to lower energies, producing a more realistic dose curve; however, the SHIELDOSE code does not. All other solar proton doses presented were calculated with the PDOSE code, since this program produces a more realistic dose curve with the input solar proton spectra produced by the solar proton models. The trapped proton results for the SHIELDOSE code did not show any discrepancy, since the lower energy limit for the trapped proton spectra was 0.5 MeV. The PDOSE program has been used extensively in Shuttle calculations and has been verified with shuttle dosimetry measurements.[7] Hence, we can conclude that SHIELDOSE produces accurate results in the proton calculation, although secondary proton effects are not included. However, depending on the proton input

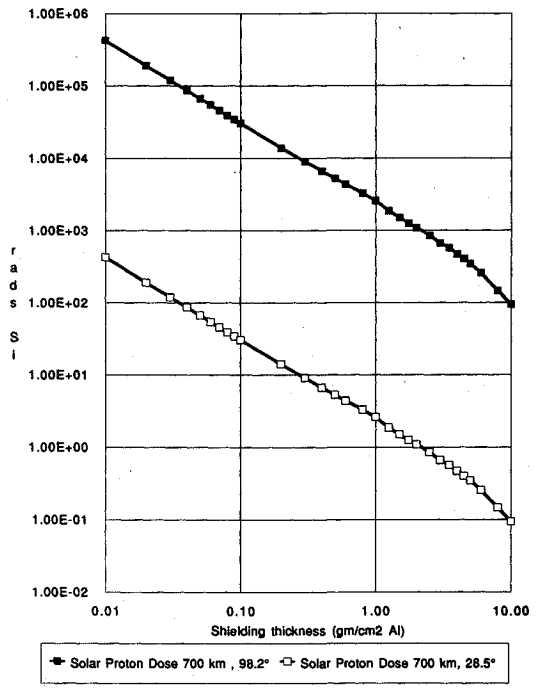

Fig. 6 Solar proton dose in a silicon target inside a solid aluminum sphere for a 5-yr mission at 700-km orbit with two different inclinations, 28.5 and 98.2 deg at solar maximum.

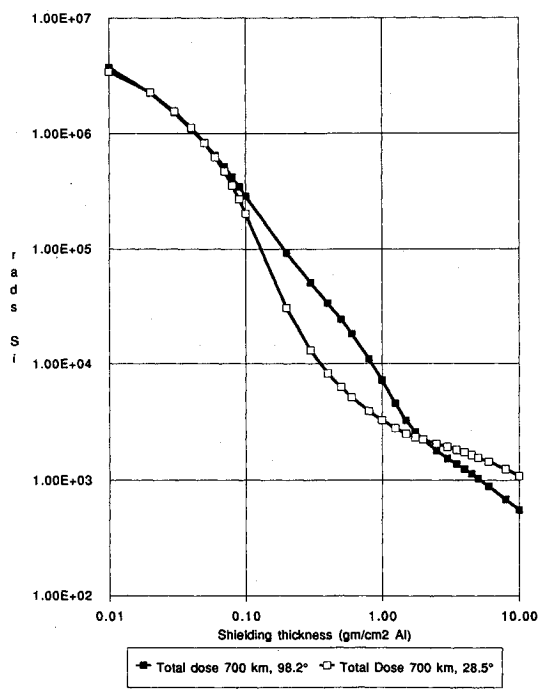

Fig. 7 Total dose in a silicon target inside a solid aluminum sphere for a 5-yr mission at 700-km orbit with two different inclinations, 28.5 and 98.2 deg at solar maximum.

spectra, appropriate caution must be used in interpreting the results at thinner shielding thicknesses. This is particularly true for orbits encountering few electrons, such as low-Earth orbits.

The two solar proton models used in this work, SPE and SOLPRO, were run for the 700-km, 98.2-deg mission beginning in June 1998, and the results are shown in Fig. 9. The fluence calculated by the two models is close for energies from 40 to 140 MeV, with the SOLPRO output being slightly greater than the SPE. In the lower and higher energy regions, however, the SPE model output is clearly higher, with the greatest difference at the 10-MeV fluence, which is almost an order of magnitude higher than that of the SOLPRO model. To see the effect of these differences on the radiation dose, the dose due to the curves in Fig. 9 is presented in Fig. 10. Here, the differences are most significantly manifest in the dose at the lower shielding thicknesses, below 1.0 gm/cm^2, beyond which the dose is very close for the fluence output of the two models. It is probable that since the SPE model incorporates more data than the SOLPRO model, it will produce more accurate results. Regardless, the SPE model predicts higher

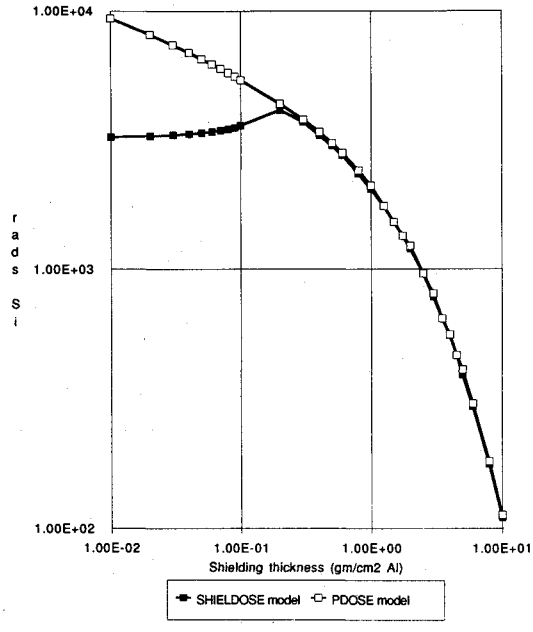

Fig. 8 Comparison of solar proton doses calculated by both the SHIELDOSE and PDOSE codes in a silicon target inside a solid aluminum sphere, for a 5-yr mission at 700-km orbit at 98.2-deg inclination at solar maximum.

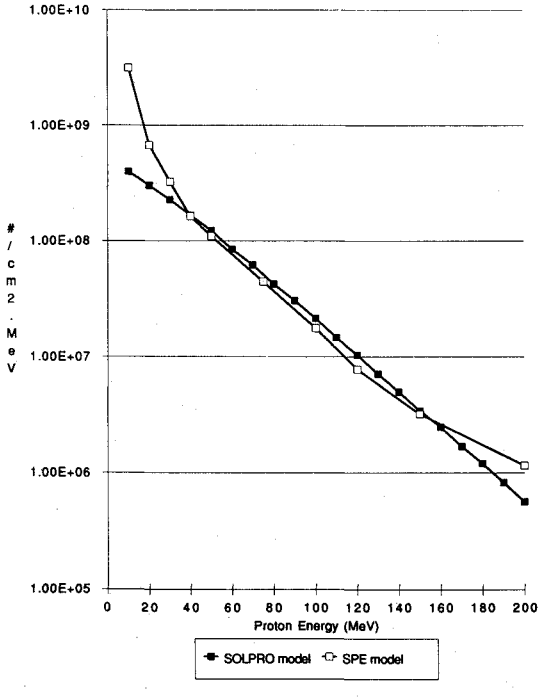

Fig. 9 Solar proton differential fluence calculated using both SPE and SOLPRO models, for a 5-yr mission at 700-km orbit at 98.2-deg inclination at solar maximum beginning in June 1998.

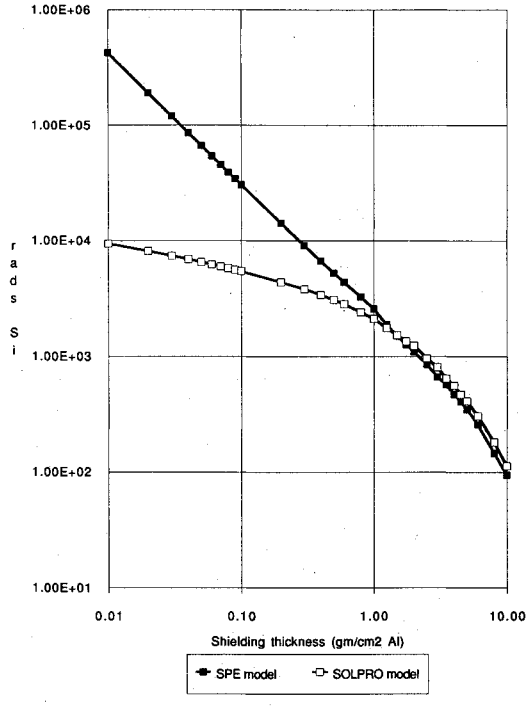

Fig. 10 Radiation dose due to solar protons using fluences from Fig. 9, in a silicon target inside a solid aluminum sphere, for a 5-yr mission at 700-km orbit at 98.2-deg inclination at solar maximum beginning in June 1998.

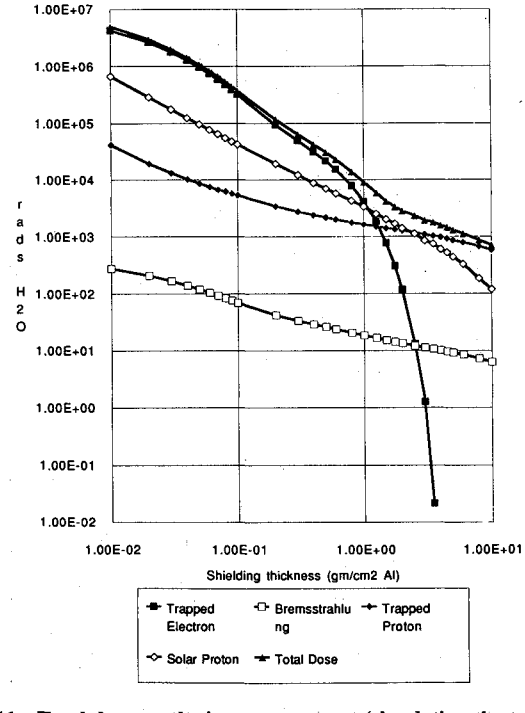

Fig. 11 Total dose results in a water target (simulating tissue) inside a solid aluminum sphere for a 5-yr polar orbit (98.2-deg inclination) at 700 km in solar maximum.

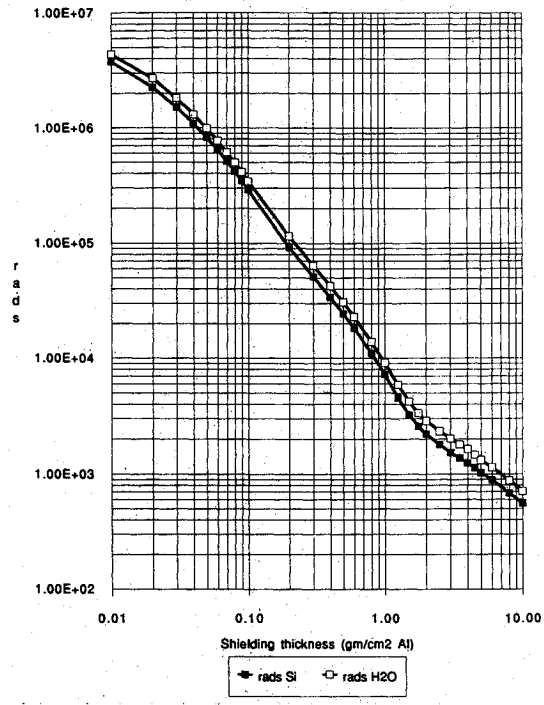

Fig. 12 Comparison of total dose in rads-water and rads-silicon inside a solid aluminum sphere for a 5-yr polar orbit (98.2-deg inclination) at 700 km in solar maximum.

integral fluences and as such provides more conservative dose estimates across the spectrum.

The final analysis was done by obtaining the dose in water at the 700-km, 98.2-deg orbit. This is done by changing only one input parameter, the units of radiation dose. Figure 11 presents the dose in rads-H_2O for each of the contributing types of radiation and the total integrated dose. It is clear that these curves are very similar to those in Fig. 2, representing the dose in rads-silicon. To better compare the two, Fig. 12 shows the total dose for the two radiation units. Note that the shape of the curve is similar, but the magnitude changes noticeably. It is important to point out that the electron and proton doses are affected differently by the incident material (as indicated by the slopes of the dose curves). The proton dose at higher shieldings is lower in water than in silicon, but for lower shieldings the dose behaves in the opposite manner. Conversely, the electron and bremsstrahlung doses are higher in water than in silicon for higher shieldings and lower for lower shieldings. These differences will become prominent in orbits that do not encounter either protons or electrons.

Conclusions

This paper presents the results of work that has incorporated several existing models of the orbital radiation environment into a single user-friendly package for rapid, accurate determination of the spacecraft mission dosage. Results are provided for silicon targets for a variety of scenarios. One calculation has been shown for water (tissue) targets. Similar results can be obtained for the radiation dose in water or aluminum. The package that has been presented is valid for elliptical orbits as well as circular orbits and includes the latest data available.It has been the intent of this paper to demonstrate the following:

1) Although current radiation analysis is a time-consuming and costly endeavor, existing radiation models can be assembled into a meaningful, usable package with short run times and user-friendly presentation.

2) Given this new tool, only limited knowledge of the space environment is required for accurate and complete mission analysis.

3) With such a package, radiation modeling can be incorporated into the space mission design process with minimal cost and planning time.

With this capability, it is more reasonable to consider incorporation of radiation dose estimates directly into the design of space missions. Prior knowledge of the radiation dosage can ultimately improve mission design, reduce mission risks, and decrease overall planning time.

It is therefore expected that the availability of a code of this type will have a wide range of applications for spacecraft design, including life support, parts analysis, shielding design, trajectory selection, and overall mass requirements.

Acknowledgments

A portion of this work was supported by the NASA Langley Research Center under the auspices of John Nealy.The authors wish to express their gratitude to several individuals who have contributed greatly to this effort, in particular, J. Nealy, Langley Research Center, S. Seltzer, National Institute of Standards and Technology, and J. Watts, Marshall Space Flight Center. In addition, we would like to thank J. Murphy and S. Gabriel, Jet Propulsion Laboratory, for providing background information, especially about the SPE model. Thanks also to D. Anna, Goddard Space Flight Center, for providing JPL and GE data for comparison, and T. Wehrung, University Research Foundation.

References

[1]Jursa, A., "Handbook of Geophysics and the Space Environment," Air Force Geophysics Lab., Air Force Systems Command, United States Air Force, 1985.

[2]Adams, J. H., Jr., Silberberg, R., and Tsao, C. H., "Cosmic Ray Effects on Microelectronics, Part I: The Near-Earth Particle Environment," Naval Research Lab., NRL Memorandum Rept. 4606, Washington, DC, Aug. 1981.

[3]Feynman, J., Armstrong, T. P., Dao-Gibner, L., and Silverman, S., "Solar Proton Events During Solar Cycles 19, 20, 21," *Solar Physics,* Vol. 126, Jet Propulsion Lab., 1990, pp. 385–401.

[4]Feynman, J., Armstrong, T. P., Dao-Gibner, L., and Silverman, S., "A New Interplanetary Proton Fluence Model," *Journal of Spacecraft and Rockets* (to be published).

[5]Burrell, M. O., and Wright, J. J., "Orbital Calculations and Trapped Radiation Mapping," NASA TM-53406, 1966.

[6]Konradi, A., Hardy, A. C., Atwell, W., "Radiation Environment Models and the Atmospheric Cutoff," *Journal of Spacecraft and Rockets,* Vol. 24, No. 3, 1987, pp. 284–285.

[7]Atwell, W., "Astronaut Exposure to Space Radiation: Space Shuttle Experience," Society of Automotive Engineers, TP 901342, Warrendale, PA, July 1990.

[8]Peddie, N. W., "International Geomagnetic Reference Field," National Space Science Data Center, Greenbelt, MD, 1985.

[9]Sawyer, D. M., and Vette, J. I., "AP8 Trapped Electron for Solar Maximum and Solar Minimum," National Space Science Data Center, NSSDC 76-06, Greenbelt, MD, Dec. 1976.

[10]Sawyer, D. M., and Vette, J. I., "AE8 Trapped Electron Model," National Space Science Data Center, Greenbelt, MD (to be published).

[11]Stassinopoulus, E. G., "SOLPRO: A Computer Code to Calculate Probabilistic Energetic Solar Proton Fluences," National Space Science Data Center, NSSDC 75-11, Greenbelt, MD, April 1975.

[12]Seltzer, S., "SHIELDOSE: A Computer Code for Space Shielding Radiation Dose Calculations," U.S. Dept. of Commerce, National Bureau of Standards, NBS TN 1116, May 1980.

Antoni K. Jakubowski
Associate Editor